Theoretical and Computational Acoustics
D. Lee, Y-H Pao, M.H. Schultz, and Y-C Teng (Editors)

Analysis of Transient Acoustic Wavefields in Continuously Layered Media with Attenuation: An Approach Based on Symbolic Manipulation

Martin D. Verweij
Laboratory of Electromagnetic Research, Department of Electrical Engineering
Centre for Technical Geoscience, Delft University of Technology
P.O. Box 5031, 2600 GA Delft, The Netherlands

Abstract: An integral transformation-type method is presented for the analysis of the space-time domain acoustic wavefield – and the associated Green's function – in a continuously layered, lossy, isotropic (equivalent) fluid. Application of a vertically varying compliance memory function makes it possible to model a large class of depth-dependent loss properties. The method combines higher-order WKBJ-like asymptotics with the Cagniard-De Hoop method of inverse transformation. The coefficients that occur in the WKBJ asymptotics follow from a recurrence scheme that is easy to evaluate by means of a symbolic manipulation program. The form of the transform domain expressions leads to a very fast inversion process. Numerical results are presented for reflections from continuously layered halfspaces with depth-dependent losses.

1. INTRODUCTION

There are a number of areas where continuously layered fluids – fluids with medium properties that change in a continuous way in the vertical direction – may be applied for modeling purposes. For ocean acoustics and underwater acoustics, their usefulness is easily recognized. In seismics, continuously layered equivalent fluid models may be employed when only the slow vertical changes of the properties of the Earth are relevant – e.g., in computational backgrounds – while at the same time it suffices to represent the solid medium by an equivalent fluid. Unlike most fluids, the internal losses in many solids are significant. For seismic applications it is therefore important that the loss behavior of a viscoelastic solid is carried over to its equivalent fluid representation. The compliance memory function (Boltzmann [1], Ben-Menahem and Singh [2]) is well suited for modeling the losses in fluids, since it can directly be incorporated in the basic acoustic equations (Verweij [3]).

For the analysis of the acoustic wavefield in media with temporal and/or spatial invariances, various integral transformation-type methods exist (Chapman and Orcutt [4]). In this paper we will develop an integral transformation-type method for the determination of the space-time domain acoustic wavefield in a continuously layered, isotropic fluid with depth-dependent losses. Its main ingredients are: a temporal Laplace transformation – with a real and positive transform parameter – followed by horizontal spatial Fourier transformations; higher-order WKBJ-like asymptotic approximations of the transform domain solution in inverse powers of the Laplace parameter; and the Cagniard-De Hoop method of inverse transformation. Since the asymptotic representations are valid for large values of the Laplace parameter, the resulting space-time domain approximations will be most accurate near the arrival time. The occurrence

of the same exponential function in all terms of the WKBJ-like asymptotic representations will enable us to organize the inverse transformation in a very efficient way. By applying higher-order asymptotics our method will often yield more accurate results – especially somewhat away from the arrival time – than with the more common zero-order or first-order asymptotic methods. As always, there will also be another side of the coin. Due to the nature of the applied asymptotics, for any finite value of the Laplace transform parameter there exists a certain order beyond which the accuracy of the transform domain asymptotic representations will no longer improve. In the space-time domain this may lead to divergence of the higher-order approximations after a configuration-dependent time instant, i.e., the method may loose its significance for later time instants. When the first arrival at the point of observation is associated with a turning ray, it will not be accounted for by the exponential function in the WKBJ-like asymptotics, and the method can not be applied.

2. CONFIGURATION AND BASIC ACOUSTIC EQUATIONS

In this paper we will determine, for a known point source at x_i^S in a known continuously layered, lossy fluid, the acoustic wavefield that is present at a point of observation at x_i^{obs}. We assume that the wavefield in this medium satisfies the linearized basic acoustic equations

$$\partial_k v_k(x_i,t) + \kappa(x_3)\,\partial_t p(x_i,t) + a(x_3,t) * p(x_i,t) = q(x_i,t), \tag{1}$$

$$\partial_k p(x_i,t) + \rho(x_3)\,\partial_t v_k(x_i,t) + b(x_3,t) * v_k(x_i,t) = f_k(x_i,t). \tag{2}$$

Here we have introduced the subscript notation and the summation convention, where the lower-case Latin subscripts (except t) range from 1 to 3. The state quantities of the acoustic wavefield are the particle velocity v_k and the acoustic pressure p. The symbols ∂_k and ∂_t denote a differentiation with respect to x_k and t, respectively. The symbol $*$ indicates a temporal convolution. The source action is described by the volume density of volume injection rate q and the volume density of volume force f_k. Without loss of generality we may assume that

$$q(x_i,t) = Q^S(t)\,\delta(x_1,x_2,x_3-x_3^S), \tag{3}$$

$$f_k(x_i,t) = F_k^S(t)\,\delta(x_1,x_2,x_3-x_3^S), \tag{4}$$

with $Q^S(t) = 0$ and $F_k^S(t) = 0$ for $t < 0$. The compressibility $\kappa(x_3)$ and the mass density $\rho(x_3)$ represent the instantaneous reaction of the medium, and the memory functions $a(x_3,t)$ and $b(x_3,t)$ represent the non-instantaneous reaction of the medium, i.e., the losses. For the after-effects in the compliance, the relation $a(x_3,t) = \partial_t^2\phi(x_3,t)$ holds, where $\phi(x_3,t)$ is the (reduced) creep function. We omit memory effects in the inertia behavior and set $b(x_3,t) = 0$, as is often done in the literature. Further we assume that $\kappa(x_3)$, $\rho(x_3)$ and $a(x_3,t)$ are continuous functions of x_3 that are as often differentiable as required by our analysis.

3. FORWARD TRANSFORMATION

We first subject the space-time domain quantities to the temporal Laplace transformation

$$\hat{p}(x_i,s) = \int_{0-}^{\infty} p(x_i,t)\,\exp(-st)\,\mathrm{d}t. \tag{5}$$

Reversely, for a given function $\hat{p}(x_i,s)$, the solution $p(x_i,t)$ of this integral equation is unique and causal if $\hat{p}(x_i,s)$ is bounded for the infinite set of points $s_n = s_0 + n\ell$ with s_0 real, positive and sufficiently large, $n = 0,1,2,\cdots$, and ℓ positive and real (Lerch's theorem, see Widder [5]).

In the Cagniard-De Hoop method only these values of s play a role. We further apply the double horizontal spatial Fourier transformation of the Radon type

$$\tilde{p}(\alpha_1, \alpha_2, x_3, s) = \int_{-\infty}^{\infty} \int_{-\infty}^{\infty} \hat{p}(x_i, s) \exp[is(\alpha_1 x_1 + \alpha_2 x_2)] \, \mathrm{d}x_1 \, \mathrm{d}x_2. \tag{6}$$

The inverse of this Fourier transformation is

$$\hat{p}(x_i, s) = \left(\frac{s}{2\pi}\right)^2 \int_{-\infty}^{\infty} \int_{-\infty}^{\infty} \tilde{p}(\alpha_1, \alpha_2, x_3, s) \exp[-is(\alpha_1 x_1 + \alpha_2 x_2)] \, \mathrm{d}\alpha_1 \, \mathrm{d}\alpha_2. \tag{7}$$

To keep the expressions readable, from now on we will omit most arguments of the functions.

Application of the forward transformations to Eqs. (1) and (2), followed by the elimination of $\tilde{v}_1$ and $\tilde{v}_2$, results in the transform domain state vector differential equation

$$\partial_3 \tilde{b}_I + sA_{IJ}(x_3) \, \tilde{b}_J = K_{IJ}(x_3, s) \, \tilde{b}_J + \tilde{u}_I. \tag{8}$$

The upper case Latin subscripts range from 1 to 2. Here, $\tilde{b}_I = (\tilde{v}_3, \tilde{p})^{\mathsf{T}}$ is the transform domain state vector, and $\tilde{u}_I = \delta(x_3 - x_3^S)(\hat{Q}^N, \hat{F}^N)^{\mathsf{T}}$ is a notional source vector with

$$\begin{pmatrix} \hat{Q}^N \\ \hat{F}^N \end{pmatrix} = \begin{pmatrix} \hat{Q}^S + i(\alpha_1 \hat{F}_1^S + \alpha_2 \hat{F}_2^S)/\rho(x_3) \\ \hat{F}_3^S \end{pmatrix}. \tag{9}$$

Further,

$$A_{IJ}(x_3) = \begin{pmatrix} 0 & \gamma(x_3) Y(x_3) \\ \gamma(x_3)/Y(x_3) & 0 \end{pmatrix} \tag{10}$$

forms the system matrix, in which $\gamma(x_3) = [c(x_3)^{-2} + \alpha_1^2 + \alpha_2^2]^{1/2}$ is the vertical slowness – with $c(x_3) = [\rho(x_3) \, \kappa(x_3)]^{-1/2}$ being the acoustic wavespeed – and $Y(x_3) = \gamma(x_3)/\rho(x_3)$ is the vertical acoustic wave admittance. The fact that $\gamma(x_3)$ is real and greater than zero for any of the values of α_1 and α_2 that occur in the inverse Fourier transformation, is important for the validity of the WKBJ-like asymptotics that will be introduced in the next section. Moreover,

$$K_{IJ}(x_3, s) = \begin{pmatrix} 0 & -\hat{a}(x_3, s) \\ 0 & 0 \end{pmatrix} \tag{11}$$

is the memory matrix representing the losses.

4. WKBJ-LIKE ASYMPTOTIC REPRESENTATIONS

As the first step in finding approximate solutions of the state vector differential equation, we introduce the wavevector $\tilde{w}_I$ through the composition relation $\tilde{b}_I = N_{IJ}(x_3) \, \tilde{w}_J$, where

$$N_{IJ}(x_3) = \tfrac{1}{2}\sqrt{2} \begin{pmatrix} Y^{1/2}(x_3) & -Y^{1/2}(x_3) \\ Y^{-1/2}(x_3) & Y^{-1/2}(x_3) \end{pmatrix}. \tag{12}$$

The wavevector components $\tilde{w}_1$ and $\tilde{w}_2$ represent waves that travel in the positive and the negative x_3-direction, respectively. Substitution of the composition relation in Eq. (8) yields the wavevector differential equation, which we subsequently recast into the corresponding integral equation (cf. Verweij [3], [6])

$$\tilde{w}_I = \mathsf{L}_{IJ} \, \tilde{w}_J + \tilde{h}_I. \tag{13}$$

The term

$$\mathsf{L}_{IJ}\,\tilde{w}_J = \begin{pmatrix} \displaystyle\int_{-\infty}^{x_3} [\Theta_{11}(x_3',s)\,\tilde{w}_1(x_3') + \Theta_{12}(x_3',s)\,\tilde{w}_2(x_3')]\,\exp(-s\textstyle\int_{x_3'}^{x_3}\gamma\,\mathrm{d}\zeta)\,\mathrm{d}x_3' \\ \\ \displaystyle -\int_{x_3}^{\infty} [\Theta_{21}(x_3',s)\,\tilde{w}_1(x_3') + \Theta_{22}(x_3',s)\,\tilde{w}_2(x_3')]\,\exp(-s\textstyle\int_{x_3'}^{x_3}\gamma\,\mathrm{d}\zeta)\,\mathrm{d}x_3' \end{pmatrix}, \tag{14}$$

with $\Theta_{IJ}(x_3,s) = [(-1)^I\,\hat{a}(x_3,s) + (1-\delta_{IJ})\,\partial_3 Y(x_3)]/2Y(x_3)$, stems from the losses and the inhomogeneity of the medium. The term

$$\tilde{h}_I = \begin{pmatrix} \frac{1}{2}\sqrt{2}\,\tilde{a}_1\,H(x_3 - x_3^S)\exp(-s\textstyle\int_{x_3}^{x_3^S}\gamma\,\mathrm{d}\zeta) \\ \\ -\frac{1}{2}\sqrt{2}\,\tilde{a}_2\,H(x_3^S - x_3)\exp(-s\textstyle\int_{x_3^S}^{x_3}\gamma\,\mathrm{d}\zeta) \end{pmatrix}, \tag{15}$$

with $\tilde{a}_i = \hat{F}_3^S\,Y^{1/2}(x_3^S) - (-1)^i\hat{Q}^S\,Y^{-1/2}(x_3^S)$, originates from the source.

Now we have to solve the wavevector integral equation. Repeated substitution of Eq. (13) into itself yields, under very general conditions, a convergent Neumann series solution. For a general inhomogeneous, lossy medium, the analytical and numerical evaluation of the higher-order terms of this series will be virtually impossible. However, repeated integration by parts of the terms of the Neumann series solution will result in WKBJ-like asymptotic expansions of the wavevector in inverse powers of s (cf. Verweij [6]). This has inspired us to approximate the wavevector by

$$\tilde{w}_I \;\sim\; \exp(-s\textstyle\int_{x_3^S}^{x_3}\gamma\,\mathrm{d}\zeta)\displaystyle\sum_{n=0}^{N} s^{-n}\,P_I^{(n)}(x_3,s), \qquad (x_3 > x_3^S), \tag{16}$$

$$\tilde{w}_I \;\sim\; \exp(-s\textstyle\int_{x_3}^{x_3^S}\gamma\,\mathrm{d}\zeta)\displaystyle\sum_{n=0}^{N} s^{-n}\,Q_I^{(n)}(x_3,s), \qquad (x_3 < x_3^S). \tag{17}$$

These are Nth-order WKBJ-like asymptotic representations of the wavevector for large values of s. The exponential parts are supposed to give the propagation of the wavefront from the source to the point of observation, and the summation parts describe the behavior of the wavefield at the point of observation after the arrival of the wavefront. The evaluation of the coefficients $P_1^{(n)}$, $P_2^{(n)}$, $Q_1^{(n)}$ and $Q_2^{(n)}$ forms the subject of the next section.

5. RECURRENCE SCHEME FOR THE COEFFICIENTS

Substitution of Eqs. (16) and (17) into Eq. (13), followed by differentiation of the equations for $\tilde{w}_2$ with respect to x_3 and collection of the terms with equal powers of s, results in an *implicit* (i.e., with the unknown quantities being defined in terms of themselves) recurrence scheme for the components of $P_I^{(n)}$ and $Q_I^{(n)}$. We find for $n = 0$

$$P_1^{(0)} \;=\; \tfrac{1}{2}\sqrt{2}\tilde{a}_1 + \int_{x_3^S}^{x_3}\Theta_{11}\,P_1^{(0)}\,\mathrm{d}x_3', \tag{18}$$

$$P_2^{(0)} \;=\; 0, \tag{19}$$

$$Q_1^{(0)} \;=\; 0, \tag{20}$$

$$Q_2^{(0)} \;=\; -\tfrac{1}{2}\sqrt{2}\tilde{a}_2 - \int_{x_3}^{x_3^S}\Theta_{22}\,Q_2^{(0)}\,\mathrm{d}x_3', \tag{21}$$

and for $n \geq 1$

$$P_1^{(n)} = \int_{x_3^S}^{x_3} [\Theta_{11} P_1^{(n)} + \Theta_{12} P_2^{(n)}] \, \mathrm{d}x_3' + Q_1^{(n)}(x_3^S), \tag{22}$$

$$P_2^{(n)} = \frac{-1}{2\gamma} [\Theta_{21} P_1^{(n-1)} + \Theta_{22} P_2^{(n-1)} - \partial_3 P_2^{(n-1)}], \tag{23}$$

$$Q_1^{(n)} = \frac{1}{2\gamma} [\Theta_{11} Q_1^{(n-1)} + \Theta_{12} Q_2^{(n-1)} - \partial_3 Q_1^{(n-1)}], \tag{24}$$

$$Q_2^{(n)} = \int_{x_3}^{x_3^S} [\Theta_{21} Q_1^{(n)} + \Theta_{22} Q_2^{(n)}] \, \mathrm{d}x_3' + P_2^{(n)}(x_3^S). \tag{25}$$

We have maintained the exact functions $\Theta_{IJ}(x_3, s)$ in this scheme because in our case it will be difficult to obtain accurate approximations of the functions $\Theta_{IJ}(x_3, s)$ in inverse powers of s within a reasonably low number of terms. This will be the case since we will employ memory functions with characteristic times that are small on the time scale that will be used for the wavefield quantities. Since the summation parts in Eqs. (16) and (17) will not only contain inverse powers of s – as with WKBJ asymptotics – but also the function $\hat{a}(x_3, s)$ and/or its derivatives $\partial_3^k \hat{a}(x_3, s)$, we have used the notion WKBJ-*like* asymptotics in this paper.

To evaluate the implicit recurrence scheme, we assume that on the closed interval between x_3^S and x_3^{obs} the functions $\Theta_{IJ}(x_3, s)$, $1/2\gamma(x_3)$ and $\Theta_{IJ}(x_3, s)/2\gamma(x_3)$ may be approximated by the following Taylor polynomials

$$\Theta_{IJ}(x_3, s) \approx \sum_{m=0}^{M} \Theta_{IJ}^{(m)}(s) \, (x_3 - x_3^S)^m, \tag{26}$$

$$\frac{1}{2\gamma(x_3)} \approx \sum_{m=0}^{M} \gamma^{(m)} \, (x_3 - x_3^S)^m, \tag{27}$$

$$\frac{\Theta_{IJ}(x_3, s)}{2\gamma(x_3)} \approx \sum_{m=0}^{M} D_{IJ}^{(m)}(s) \, (x_3 - x_3^S)^m. \tag{28}$$

Now our goal is to find approximate expressions for $P_I^{(n)}$ and $Q_I^{(n)}$ in the form of Taylor polynomials like

$$P_I^{(n)}(x_3, s) = \sum_{\ell=0}^{L} P_I^{(n,\ell)}(s) \, (x_3 - x_3^S)^\ell. \tag{29}$$

Substitution of Eqs. (26) - (29) into Eqs. (18) - (25) and collection of the terms with equal powers of $(x_3 - x_3^S)$ leads to an *explicit* (i.e., with the unknown quantities being defined only in terms of known quantities) recurrence scheme for the coefficients $P_1^{(n,\ell)}$, $P_2^{(n,\ell)}$, $Q_1^{(n,\ell)}$ and $Q_2^{(n,\ell)}$. For $n = 0$ we obtain

$$P_1^{(0,\ell)} = \left\{ \begin{array}{ll} \frac{1}{2}\sqrt{2}\, \tilde{a}_1, & (\ell = 0) \\ \\ \frac{1}{\ell} \sum_{m=0}^{\ell-1} \Theta_{11}^{(m)} P_1^{(0,\ell-m-1)}, & (\ell \geq 1) \end{array} \right\}, \tag{30}$$

$$P_2^{(0,\ell)} = 0, \qquad (\ell \geq 0), \tag{31}$$

$$Q_1^{(0,\ell)} = 0, \qquad (\ell \geq 0), \tag{32}$$

$$Q_2^{(0,\ell)} = \left\{ \begin{array}{ll} -\frac{1}{2}\sqrt{2}\,\tilde{a}_2, & (\ell = 0) \\ \frac{-1}{\ell} \sum_{m=0}^{\ell-1} \Theta_{22}^{(m)}\, Q_2^{(0,\ell-m-1)}, & (\ell \geq 1) \end{array} \right\}, \tag{33}$$

and for $n \geq 1$ we get

$$P_1^{(n,\ell)} = \left\{ \begin{array}{ll} Q_1^{(n,0)}, & (\ell = 0) \\ \frac{1}{\ell} \sum_{m=0}^{\ell-1} \Theta_{11}^{(m)}\, P_1^{(n,\ell-m-1)} + \Theta_{12}^{(m)}\, P_2^{(n,\ell-m-1)}, & (\ell \geq 1) \end{array} \right\}, \tag{34}$$

$$P_2^{(n,\ell)} = \sum_{m=0}^{\ell} [-D_{21}^{(m)}\, P_1^{(n-1,\ell-m)} - D_{22}^{(m)}\, P_2^{(n-1,\ell-m)} + (\ell - m + 1)\,\gamma^{(m)}\, P_2^{(n-1,\ell-m+1)}], \qquad (\ell \geq 0), \tag{35}$$

$$Q_1^{(n,\ell)} = \sum_{m=0}^{\ell} [D_{11}^{(m)}\, Q_1^{(n-1,\ell-m)} + D_{12}^{(m)}\, Q_2^{(n-1,\ell-m)} - (\ell - m + 1)\,\gamma^{(m)}\, Q_1^{(n-1,\ell-m+1)}], \qquad (\ell \geq 0), \tag{36}$$

$$Q_2^{(n,\ell)} = \left\{ \begin{array}{ll} P_2^{(n,0)}, & (\ell = 0) \\ \frac{-1}{\ell} \sum_{m=0}^{\ell-1} \Theta_{21}^{(m)}\, Q_1^{(n,\ell-m-1)} + \Theta_{22}^{(m)}\, Q_2^{(n,\ell-m-1)}, & (\ell \geq 1) \end{array} \right\}. \tag{37}$$

It is easy to evaluate this recurrence scheme using a symbolic manipulation program.

6. INVERSE TRANSFORMATION

To elucidate the application of the Cagniard-De Hoop method, as an example we will show here how to find the space-time domain acoustic pressure below a source of volume injection. First we remark that the coefficients $\Theta_{IJ}^{(m)}$, $\gamma^{(m)}$ and $D_{IJ}^{(m)}$ consist of terms that contain integer inverse powers of $\gamma(x_3^S)$. In many of these terms the memory function $\hat{a}(x_3^S, s)$ and/or its derivatives $\partial_3^k \hat{a}(x_3^S, s)$ occur as well. Further, in the present case we find that $\tilde{a}_1 = -\tilde{a}_2 = Y^{-1/2}(x_3^S)\,\hat{Q}^S$. From Eqs. (30) - (37) it then follows that $P_1^{(n,\ell)}$ and $P_2^{(n,\ell)}$ are composed of terms of the form $C_1\,\hat{Q}^S\,\hat{\Pi}(s)\,Y^{-1/2}(x_3^S)\,\gamma^{-\eta}(x_3^S)$. Here C_1 indicates a real constant, the function $\hat{\Pi}(s)$ stands for a certain product of the memory function and/or several of its derivatives, and η is a nonnegative integer. Upon applying the composition relation and Eqs. (16) and (29), we find that the terms of $\tilde{p}$ are of the form

$$\tfrac{1}{2} C_2\,\hat{Q}^S\,(x_3^{\rm obs} - x_3^S)^\ell\, s^{-n}\,\hat{\Pi}(s)\,Y^{-1/2}(x_3^S)\,Y^{-1/2}(x_3^{\rm obs})\,\gamma^{-\eta}(x_3^S)\,\exp(-s\textstyle\int_{x_3^S}^{x_3^{\rm obs}} \gamma\,{\rm d}\zeta), \tag{38}$$

in which C_2 is a real constant and ℓ and n are nonnegative integers. At this stage it is convenient to write $\tilde{p} = s^2 \hat{Q}^S \tilde{G}$. The Green's function $\tilde{G}$ is the acoustic pressure that is generated by a

source with a unit ramp signature Q^S. This Green's function is composed of a number of terms of the form $C_3\, s^{-n}\, \hat{\Pi}(s)\, \tilde{\Upsilon}(\eta)$, with

$$\tilde{\Upsilon}(\eta) = \tfrac{1}{2} s^{-2}\, Y^{-1/2}(x_3^S)\, Y^{-1/2}(x_3^{\rm obs}) \gamma^{-\eta}(x_3^S) \exp(-s \int_{x_3^S}^{x_3^{\rm obs}} \gamma \, {\rm d}\zeta). \tag{39}$$

The constant C_3 contains all products $C_2(x_3^{\rm obs} - x_3^S)^\ell$ of the terms of the form (38) with corresponding n, $\hat{\Pi}(s)$ and η. When higher-order asymptotics are involved, the task of finding the constants C_3 and each of the possible combinations of n, $\hat{\Pi}(s)$ and η, is almost impossible to carry out by hand, but forms no problem for a symbolic manipulation program.

The function $\tilde{\Upsilon}(\eta)$ that shows up in each term of $\tilde{G}$ is the only factor that depends on s as well as on α_1 and α_2, and only for the inversion of this part we need to employ the Cagniard-De Hoop method (see Verweij and De Hoop [7] for a description of this method in case of continuously layered media). In all cases in which our WKBJ-like asymptotics are useful, the result of this process is

$$\Upsilon(\eta) = \frac{1}{2\pi^2} H(t - T_{\rm arr}) \int_0^{Q(t)} {\rm Im} \left\{ \bar{Y}^{-1/2}(x_3^S) \bar{Y}^{-1/2}(x_3^{\rm obs}) \bar{\gamma}^{-\eta}(x_3^S)\, \partial_t p \right\} {\rm d}q, \tag{40}$$

Here, p denotes a (complex) horizontal slowness that satisfies

$$t = pr + \int_{x_3^S}^{x_3^{\rm obs}} \bar{\gamma}(\zeta) \, {\rm d}\zeta = {\rm real}. \tag{41}$$

In both foregoing equations the bar indicates that the vertical slowness has been changed into $\bar{\gamma}(x_3) = [c^{-2}(x_3) - p^2 + q^2]^{1/2}$. The points p that are relevant in view of the Cagniard-De Hoop method form a so-called Cagniard contour in the complex p-plane. The value of t associated with the point where a Cagniard contour crosses the real p-axis is indicated by $T(q)$; the unique inverse of this function for $q \geq 0$ is denoted by $Q(t)$. The quantity $T_{\rm arr} = T(0)$ is the arrival time of the wave front.

The other factors in the terms of $\tilde{G}$ solely depend on s. The inversion of s^{-n} is obtained by inspection. The time domain function $\Pi(t)$ is recognized as the convolution of the relevant time domain memory functions $a(x_3^S, t)$ and/or its derivatives $\partial_3^k a(x_3^S, t)$, which are known from the start. Convolution of the space-time domain counterparts of the factors of each term of $\tilde{G}$ yields the corresponding contribution to the space-time domain Green's function G. Once this function has been found, the space-time domain acoustic pressure follows as $p = \partial_t^2 [Q^S * G]$.

7. NUMERICAL RESULTS

In this section we will present results for the space-time domain acoustic wavefield in a simplified version of a marine seismic configuration. The quantity of interest is the acoustic pressure, and the point source is of the volume injection type. The configuration consist of a homogeneous, lossless upper halfspace (water; the effects of the surface are discarded) and an inhomogeneous and/or lossy lower halfspace (subsurface geology). This type of configuration leads to an analysis that is somewhat simpler than the one presented in the previous sections [we may replace the Taylor polynomials in Eqs. (26) - (29) by Taylor polynomials in $(x_3 - x_3^{\rm int})$, and it suffices to set $M = N - 1$ in Eqs. (26) - (28) and $L = 0$ in Eq. (29)]. The acoustic wave is generated by a source with $x_3^S = 50$ m, it reflects from the interface between the halfspaces at $x_3^{\rm int} = 100$ m, and it is observed at a receiver with $x_3^{\rm obs} = 0$ m and with the same horizontal position as the source. The medium parameters are given in Fig. 1. To describe the losses of

the equivalent fluid in the lower halfspace, we introduce the causal creep function

$$\phi(x_3,t) = \kappa(x_3)\Delta(x_3)[\gamma_{\text{euler}} + \mathrm{E}_1(\omega_0 t) + \ln(\omega_0 t)]\, H(t), \tag{42}$$

in which $\Delta(x_3) = 2/\pi Q_0(x_3)$. The symbol E_1 denotes the exponential integral. The amount of loss at a certain level x_3 is inversely proportial to the value of $Q_0(x_3)$. For angular frequencies lower than ω_0, the value of the quality factor Q of the medium is almost frequency independent and approximates $Q_0(x_3)$. This frequency behavior of Q makes that the applied creep function is well-suited for modeling the losses occurring in many types of rock. Further, a source signature is applied for which it suffices to take $\omega_0 = 200$ rad/s.

Several approximate Green's functions are depicted in Figure 2, in which the trivial step-function contribution of the direct wave has been omitted. The value of N indicates the order of the asymptotic representation. We see that before $t = 1.5$ s (unshaded region) the differences between the subsequent higher-order approximations decrease: for $N \geq 3$ they are even indistinguishable. We assume that as soon as the latter is the case, the exact Green's function is arrived at. However, beyond $t = 1.5$ s (shaded region) the subsequent approximations diverge. The fact that useful results are generated only up till a specific time instant is a consequence of the application of WKBJ-like asymptotics and determines the applicability of the method in each specific case. When there are turning rays traveling below the interface that arrive earlier than the rays reflecting at the interface, the first arrival will not be accounted for by the exponential function in the asymptotics. If this happens, divergence will occur for any time instant.

We can define two other media by either assuming the losses to be absent in the lower halfspace ($Q_0 = \infty$), or by taking the values of the wavespeed and the mass density in the lower halfspace equal to those of the upper halfspace. The Green's functions for the media thus defined are given in Fig. 3. We observe that near the arrival time the effect due to the inhomogeneity of the wavespeed and mass density is opposite to the effect due to the losses. This also follows from Fig. 4, which shows the reflected acoustic pressures in the three media for a source with a four-point optimum Blackmann signature of 0.1 s duration and unit amplitude.

8. CONCLUSIONS

In this paper we have derived a method for the determination of the space-time domain acoustic wavefield – and the corresponding Green's function – in a continuously layered, lossy, isotropic fluid or equivalent fluid. By using a depth dependent compliance memory function, intricate losses may be modeled. The form of the transform domain WKBJ-like asymptotic representations has enabled us to employ the Cagniard-De Hoop method in a very efficient way. We have tackled the problem of performing tasks that are almost impossible to carry out by hand, like the generation of the coefficients of the asymptotic representations, by invoking a symbolic manipulation program.

Typical numerical results have been generated for acoustic wavefields that are reflected by continuously layered halfspaces with a depth-dependent loss behavior. For a zero horizontal offset we have observed that there is an interval, beginning with the arrival time, on which the differences between the approximate Green's functions with increasing orders become invisibly small. In general, for later time instants the subsequent approximations diverge. The method is applicable for nonzero horizontal offsets, but becomes invalid when the first arrival at the point of observation is associated with a turning ray. We have shown numerically that near the arrival time the effect of the losses can counteract the effect of the inhomogeneity of the wavespeed and mass density.

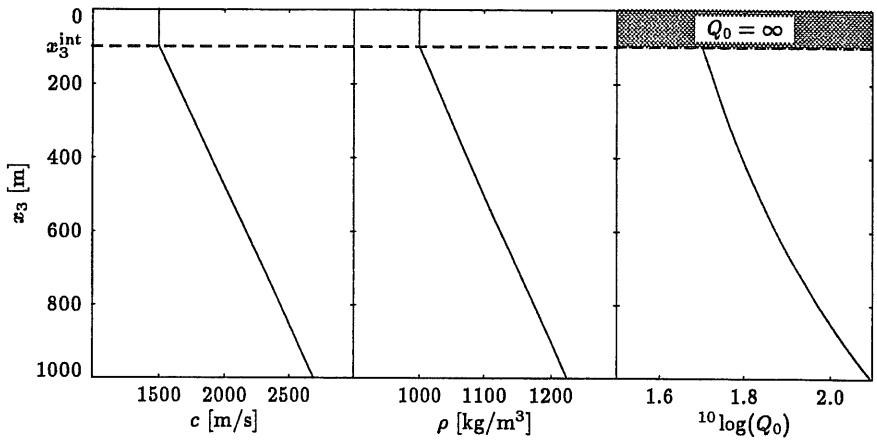

Figure 1: The depth dependence of the wavespeed c, the mass density ρ, and the parameter Q_0, as used in the example configuration.

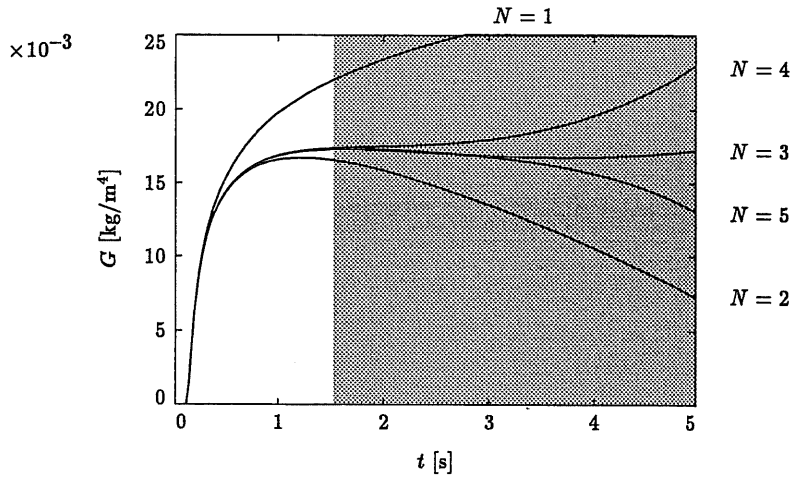

Figure 2: Several approximate Green's functions G. For $t \leq 1.5$ s the differences between the subsequent higher-order approximations decrease (unshaded region), while for $t > 1.5$ s the subsequent approximations diverge (shaded region).

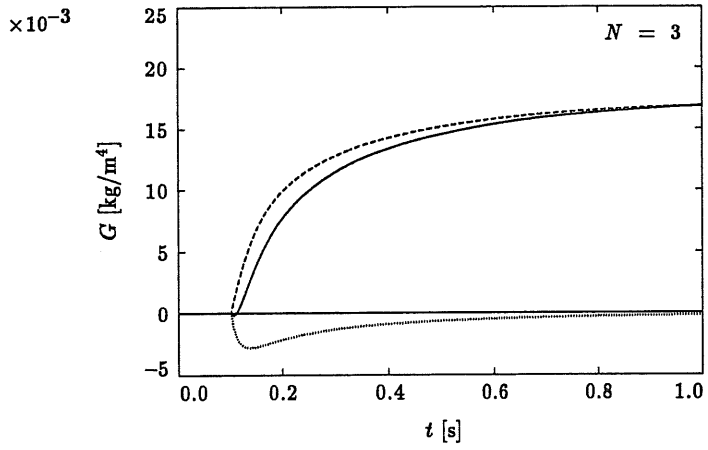

Figure 3: The Green's functions G for the original medium (solid line), a medium with the same wavespeed and mass density as the original medium but without losses (dashed line), and a medium with the same losses as the original medium but with the constant wavespeed $c = 1500$ m/s and the constant mass density $\rho = 1000$ kg/m^3 (dotted line).

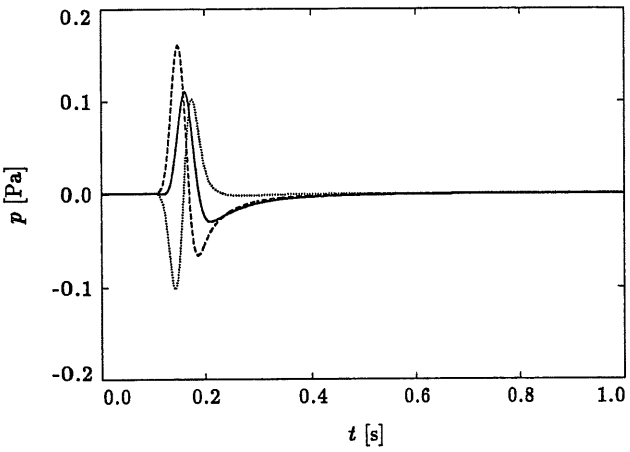

Figure 4: The acoustic pressures p for the original medium (solid line), a medium with the same wavespeed and mass density as the original medium but without losses (dashed line), and a medium with the same losses as the original medium but with the constant wavespeed $c = 1500$ m/s and the constant mass density $\rho = 1000$ kg/m^3 (dotted line).

ACKNOWLEDGMENTS

The research of the author has been made possible by a fellowship of the Royal Netherlands Academy of Arts and Sciences. The research reported in this paper has been financially supported through research grants from the Stichting Fund for Science, Technology and Research (a companion organization to the Schlumberger Foundation in the U.S.A.).

REFERENCES

[1] Boltzmann, L., Zur Theorie der elastischen Nachwirkung, Sitzber. Kaiserl. Akad. Wiss. Wien, Math.-Naturw. Kl., vol. 70(II), 1874, pp. 275-306.

[2] Ben-Menahem, A., and Singh, S. J., Seismic waves and sources, Springer-Verlag New York, Inc., New York, 1981.

[3] Verweij, M. D., Modeling space-time domain acoustic wave fields in media with attenuation: The symbolic manipulation approach, J. Acoust. Soc. Am., vol. 97, 1995, pp. 831-843.

[4] Chapman, C. H., and Orcutt, J. A., The computation of body wave synthetic seismograms in laterally homogeneous media, Rev. Geophys., vol. 23(2), 1985, pp. 105-163.

[5] Widder, D. V., The Laplace transform, Princeton Univ. Press, Princeton, 1946.

[6] Verweij, M. D., Transient acoustic wave modeling: Higher-order Wentzel-Kramers-Brillouin-Jeffreys asymptotics and symbolic manipulation, J. Acoust. Soc. Am., vol. 92, 1992, pp. 2223-2238.

[7] Verweij, M. D., and De Hoop, A. T., Determination of seismic wavefields in arbitrarily continuously layered media using the modified Cagniard method, Geophys. J. Int., vol. 108, 1990, pp. 731-754.